Joannie W. Chin,[1] *Tinh Nguyen,*[2] *and Khaled Aouadi,*[3]

Effects of Environmental Exposure on Fiber-Reinforced Plastic (FRP) Materials Used in Construction

ABSTRACT: A major hindrance to the acceptance of polymer composites in civil engineering applications is the susceptibility of the polymeric matrix to weathering. The polymer matrix is prone to degradation initiated by ultraviolet (UV) radiation, moisture, temperature, and high pH environments. The objective of this study was to characterize chemical and physical changes in polymeric matrix resins following exposure to these environments. The ultimate goal is to identify factors that contribute to matrix resin degradation under environmental and mechanical stresses.

Resin systems studied included vinyl ester and isophthalic polyester, both of which are commonly used in construction applications. Neat polymer films were exposed to UV radiation, moisture, alkaline, and saline environments. Diffusion of water, alkali, and saline solution into the polymers was calculated from gravimetric measurements. Changes in strength, viscoelastic response, and thermal properties were evaluated through tensile testing, dynamic mechanical thermal analysis (DMTA), and differential scanning calorimetry (DSC). Atomic force microscopy (AFM) and X-ray photoelectron spectroscopy (XPS) were also used for detecting changes in the polymer surface following UV exposure.

KEY WORDS: alkaline conditions, building technology, composites, durability, polyester, moisture, saline conditions, vinyl ester, ultraviolet radiation

With the continuous deterioration of the world's infrastructure, it has become increasingly urgent to determine the feasibility of using high-performance polymer composite materials in fabricating new structures as well as rehabilitating existing ones. For example, it is currently estimated that, in the U.S. transportation infrastructure alone, 13 000 interstate, 36 000 arterial, and over 45 000 collector system bridges are considered to be in deficient condition [1]. Total repair costs for corroded steel and concrete structures in the United States exceed $250 billion per year [2,3]. Additional repair and retrofitting costs for seismically deficient structures, deteriorating civil and military waterfronts, and substandard transportation infrastructure run into additional billions of dollars annually [3].

[1] Materials research engineer, National Institute of Standards and Technology, Building 226, Room B350, Gaithersburg, MD 20899.
[2] Physical scientist, National Institute of Standards and Technology, Building 226, Room B350, Gaithersburg, MD 20899.
[3] Visiting scientist, Institut des Sciences et Techniques de l'Iingenieur de Lyon, Villeurbanni, France.

In light of these sobering statistics, the Civil Engineering Research Foundation (CERF) has recommended the use of high-performance materials and systems in construction, citing potentially substantial cost savings due to lower mass of materials, reduced maintenance, and longer lifetimes [4]. The advantages that fiber-reinforced polymer composites offer over traditional building materials such as steel and concrete have been widely recognized and include a high strength/weight ratio, excellent corrosion and chemical resistance, transparency to electromagnetic radiation, and resistance to fatigue.

The polymer matrix in a fiber-reinforced composite binds and orients reinforcing fibers to carry the intended loads, protects them from handling and environment, and provides all of the interlaminar shear strength of the composite. However, the matrix is often considered to be the weak link in a fiber-reinforced composite system, since it may undergo physical damage and chemical degradation during environmental exposure and stress application. Polymer composites in outdoor applications are susceptible to photo-initiated oxidation leading to surface degradation [5,6] and are also known to be sensitive to moisture-induced damage [7,8]. Polymer composites are also touted for use as replacements for steel reinforcing bars in concrete, a highly alkaline environment, as well as for incorporation into off-shore and marine structures [9–11].

The durability of polymer composites in the environments described previously is one of the primary issues limiting the acceptance of these materials in infrastructural applications. At the present time, few studies have been conducted on the effect of moisture, saline and alkaline environments on vinyl ester and polyester properties. In addition, the combined effects of moisture, UV, and loading are also not well-documented. It is necessary to understand the mechanisms that govern polymer degradation, not only to optimize material properties, but to provide information for use in accelerated aging tests.

The objective of this research was to systematically study chemical and mechanical changes in polymer matrix composites following exposure to UV, moisture, alkaline, and saline conditions. The long-term goal is to identify factors that contribute to matrix resin degradation under environmental and mechanical stresses, a phenomenon that is of major concern in the application of composites in construction.

Experimental

Materials

Representative commercial epoxy vinyl ester and isophthalic polyester (isopolyester) resins were selected for this study. Both

systems are thermosetting materials that are suitable for fabricating fiber-reinforced composites through pultrusion and resin transfer molding processes. A typical epoxy vinyl ester consists of a bisphenol A epoxy backbone with terminal methacrylate functionality. The isopolyester resin is produced from the reaction of isophthalic acid, a glycol, and maleic anhydride. Both the vinyl ester and isopolyester resins are dissolved in styrene monomer, which also participates in free radical reactions with the resin to form the final cross-linked network.

Specimen Preparation

Vinyl ester specimens were prepared by hand-mixing the resin, 3% by mass of a methyl ethyl ketone peroxide (MEKP) catalyst containing 9% active oxygen, and a small amount (less than 0.5% by mass) of a silicone defoaming agent until thoroughly blended. A similar procedure was followed for the isopolyester specimens, except that only 2% by mass of the MEKP catalyst and no silicone defoamer were used. Because both the vinyl ester and isopolyester resins were pre-promoted and pre-accelerated, that is, the promoter and accelerator have already been added by the manufacturer, only the addition of the catalyst was necessary.

Free films for dynamic mechanical thermal analysis (DMTA), differential scanning calorimetry (DSC), atomic force microscopy (AFM), X-ray photoelectron spectroscopy (XPS), and weight uptake studies were produced by molding between two acrylic plates. Poly(ethylene terephthalate) films served as release sheets and spacers to control film thickness. Films were allowed to gel at room temperature, followed by a 2 h/150°C post-cure. Film thicknesses ranged from 230 to 260 μm.

Tensile dogbone-shaped specimens were produced for mechanical testing in a custom-designed mechanical testing device. The procedure for making dogbones is similar to that described above for films, except that a 1.5-mm thick poly(tetrafluoroethylene) dogbone mold is used. Dimensions of the dogbones are shown in Fig. 1.

Exposure Environments

Free films and dogbone specimens were immersed in distilled water, salt water (to simulate a marine or offshore environment), and an artificial concrete pore solution (to simulate the alkaline interior of a cementitious material, as would be encountered by reinforcing bars) for 1300 h at ambient temperature. The salt water solution was composed of a mass fraction of 3.5% by mass NaCl in distilled water. Concrete pore solution was formulated according to the procedure of Christensen et al. and is composed of 1.8% by mass KOH, 0.68% by mass NaOH, and 0.5% by mass $Ca(OH)_2$ in distilled water [12]. This solution has a pH of approximately 13.5. After immersion, samples were dried for 1 week under vacuum at 35°C prior to DMTA, DSC, and tensile measurements.
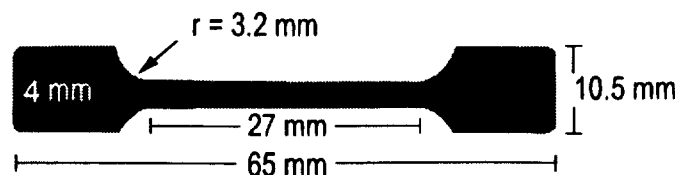

FIG. 1—*Schematic of dogbone specimen used for mechanical testing.*

Sorption Studies

25- by 25-mm polymer films were immersed in distilled water, salt water, and in concrete pore solution in individual glass screw-top jars at an ambient temperature of 22°C ± 1°C. Films were periodically removed from the solution, rinsed with distilled water (in the case of salt water and concrete pore solutions), surface dried, and weighed on a Mettler AT automatic balance.[4] The rate of water and solution sorption was measured as the rate of weight change, referenced to the initial dry weight of the film. Six films of each polymer were tested in each solution.

For uptake studies at 60°C, the procedure is similar to the one described above with the exception that the screw-top jars are placed in a sand bath maintained at 60°C. Mass uptake was determined as previously described.

Ultraviolet Irradiation

10- by 15-cm polymer films with an approximate thickness of 250 μm were exposed to a 1000 W xenon arc source for 1200 h in an Oriel solar simulator. The temperature in the specimen chamber during the exposure period was maintained at 30°C. Intensity of the 250 to 820 nm output was measured to be 25 W/(m²·nm) at 350 nm.

Thermal Analysis

Differential Scanning Calorimetry (DSC)—12 to 15 mg samples of polymer were sealed in aluminum pans and analyzed in a DSC 2910 (TA Instruments) differential scanning calorimeter equipped with a refrigerated cooling system. Analysis was conducted in modulated DSC mode, with a modulation frequency of +/−1.0°C per 60 s. Samples were ramped from 25 to 180°C at a heating rate of 5.0°C/min. Two to three samples were analyzed for each polymer and each exposure condition.

Dynamic Mechanical Thermal Analysis (DMTA)—12- by 35-mm films were tested in tensile mode in a Rheometrics solids analyzer (RSA) II, at a frequency of 10 Hz and 0.05% strain. Film thicknesses ranged from 230 to 330 μm. Analysis was carried out from 30 to 180°C, with data being recorded in 2°C increments. Samples were pre-strained to maintain a constant state of tension throughout the experiment and to prevent film buckling. Three samples of each polymer were analyzed for each exposure condition.

Tensile Testing

The testing device used for determining mechanical properties consisted of a screw-driven linear actuator equipped with a 227 kg (500 lb) load cell and linear voltage displacement transducer (LVDT). Samples were secured in machined aluminum grips that conformed exactly to the shape of the end tabs. Specimens were loaded at the rate of 1 mm/s at room temperature. Load and displacement data from the load cell and LVDT were continually recorded by a computer during the course of the experiment. Three

to five samples were tested for each polymer and exposure condition.

X-Ray Photoelectron Spectroscopy

X-ray photoelectron spectroscopy (XPS) analysis was carried out on a Perkin-Elmer PHI 5400 spectrometer equipped with a MgK_α achromatic X-ray source (1253.6 eV), operating at 14 keV and 300 W with an emission current of 25 mA. Pressure inside the ultra-high vacuum chamber was maintained around 10^{-6} Pa during the course of analysis. Dimensions of the analyzed areas were typically 1.1 by 3.3 mm.

Binding energies for all observed photopeaks were referenced to the value of the carbon-carbon/carbon-hydrogen bond at 285 eV. Atomic concentration calculations and curve-fitting were carried out using PHI software version 4.0.

Atomic Force Microscopy (AFM)

AFM images were obtained in tapping mode on a Digital Instruments Dimension 3000 AFM. Dimensions of the scanned areas were approximately 15 by 15 μm. Z-axis resolution was typically 100 to 300 nm.

Results and Discussion

Water and Solution Uptake

Most polymers are known to take up several percent of water by mass, depending on their chemical composition. The equilibrium and rate of sorption are of interest because they strongly influence both the thermophysical properties and viscoelastic response of polymer composites. Extensive studies in this area by a number of researchers have been compiled by Springer [13]. Since salt water and concrete pore solution are also aqueous, the sorption behavior of the vinyl ester and isopolyester materials in these environments is also of interest. Obviously, the main difference between water and the other two solutions of interest is the presence of electrolytes, which may interact with the polymers.

As shown by Figs. 2 through 5, a quasi-equilibrium state is reached in both polymers in all three immersion solutions and at
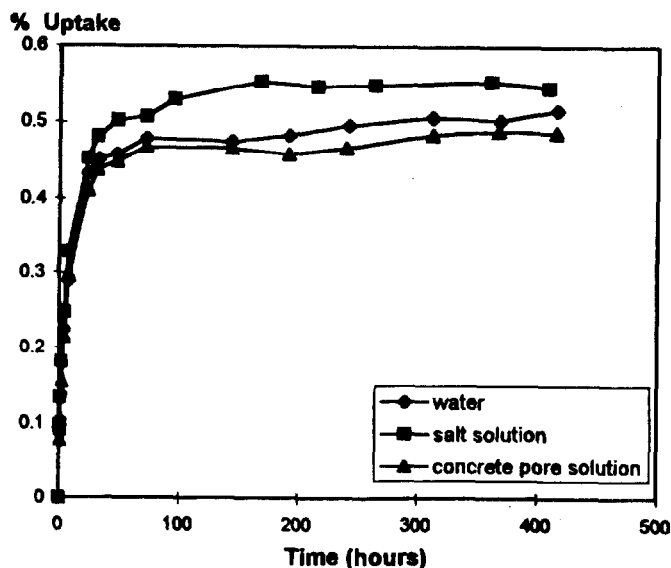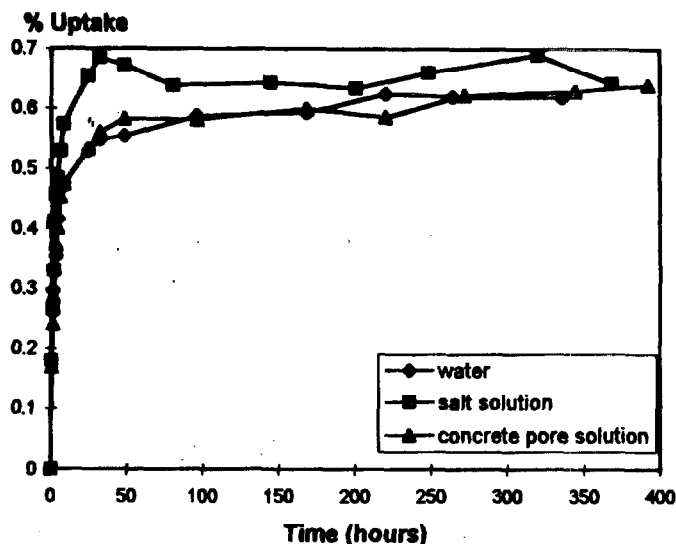

FIG. 3—*Uptake of distilled water, salt solution, and concrete pore solution for vinyl ester at 60°C (standard deviation of data is typically 0.02 to 0.03%).*

both temperatures well before 50 h have elapsed. The relative standard deviation of the data is typically 0.02 to 0.03%. However, it appears that sorption takes place at a higher rate for the samples held at 60°C and that the equilibrium quantity sorbed is also slightly higher. Comparison between the results of the ambient temperature and 60°C immersions is helpful in determining the validity of accelerated aging schemes involving the use of elevated temperatures.

For the vinyl ester materials at both ambient temperature and 60°C, Figs. 2 and 3 show that total salt water uptake is higher than that of water or pore solution. Up to 400 h, sorption of water, salt solution, and concrete pore solution remains relatively constant for both exposure temperatures.

This same sorption pattern is observed for isopolyester at ambient temperature, as shown in Fig. 4. In the case of isopolyester at
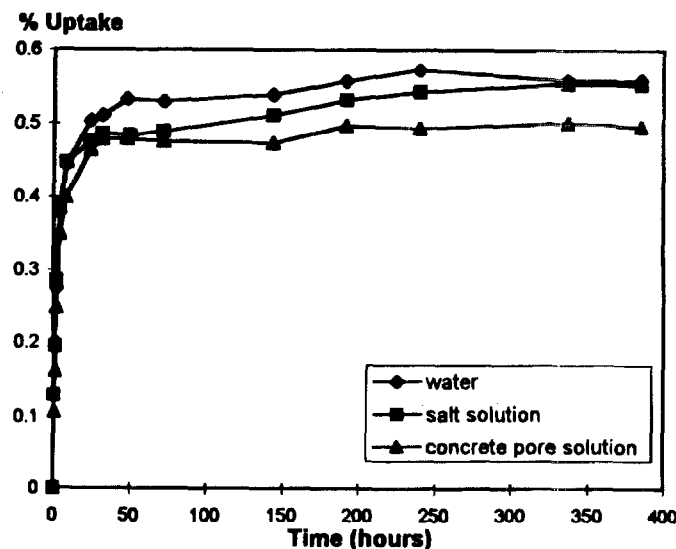

FIG. 2—*Uptake of distilled water, salt solution, and concrete pore solution for vinyl ester at 22°C (standard deviation of data is typically 0.02 to 0.03%).*

FIG. 4—*Uptake of distilled water, salt solution, and concrete pore solution for isopolyester at 22°C (standard deviation of data is typically 0.02 to 0.03%).*
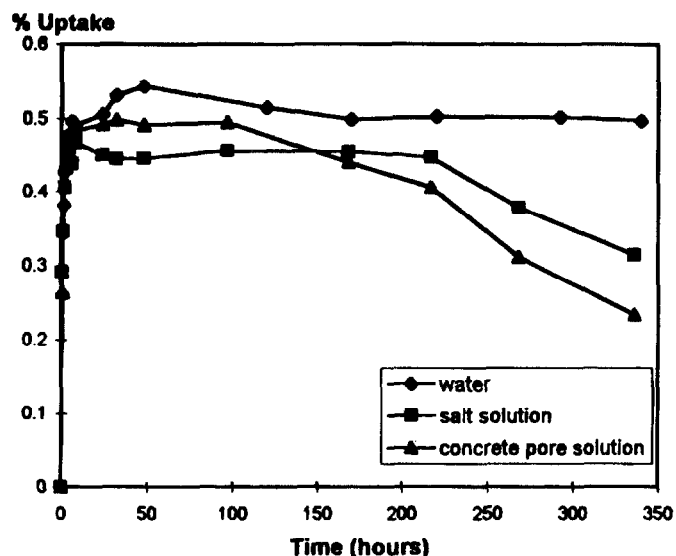
FIG. 5—*Uptake of distilled water, salt solution, and concrete pore solution for isopolyester at 60°C (standard deviation of data is typically 0.02 to 0.03%).*

60°C, however, significant differences in sorption behavior are seen, as depicted in Fig. 5. In the concrete pore solution and salt solution immersions, mass loss begins to occur, after 100 h for the pore solution and after 200 h for the salt solution. This observation points to the possibility of polymer breakdown followed by the leaching of soluble degradation or hydrolysis products. Obviously, not only high pH but also cations are involved in the hydrolysis of the isopolyester. Comparison of Figs. 4 and 5 strongly indicate that temperature is another key factor in the degradation of isopolyester. Morri et al. have also observed mass losses following hygrothermal exposure for glass fiber-reinforced polyesters, which was attributed to resin degradation [14].

The observation that no significant mass loss was observed for vinyl ester in any solution even at 60°C is consistent with the belief that vinyl esters are more stable to hydrolysis than isopolyester. Ester linkages in vinyl esters are terminal and are shielded by methyl groups. In most polyesters, ester groups are distributed along the main chain, making them more available (and hence more vulnerable) to hydrolysis reactions.

The question of whether ions from solution actually diffuse into the resin remains to be answered and is the subject of a study currently underway in our lab. A study by Katsuki and Uomoto discussed the use of electron probe analysis to analyze fiber-reinforced vinyl ester rods following a 60-day immersion in 2 mol/L NaOH solution [15]. Their results showed that sodium ions penetrated into the rods through the exterior resin layer. However, it is not clear if the sodium ions actually diffused through the resin or if penetration was made through surface defects and then along fiber interfaces.

Thermal Analysis, DSC, DMTA

The glass transition temperature T_g is not only an indicator of the thermal stability of a material, but is also closely tied to polymer structure and mechanical properties [16]. Figures 6 and 7 show comparisons of T_gs of the dried vinyl ester and isopolyester films following the various exposures at ambient temperature after 1300 h. The glass transition temperature was taken to be the peak of
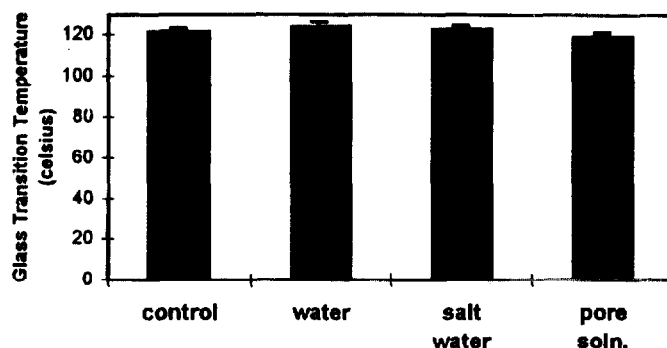

FIG. 6—*Glass transition temperature* T_g *of vinyl ester samples measured by dynamic mechanical thermal analysis (DMTA) after 1300 h of immersion in water, salt solution, and concrete pore solution at ambient temperature (uncertainty is equal to ±1 standard deviation).*

the loss modulus (E″) curve. No significant differences were observed in the T_g or in the value of the storage modulus (E′) in the glassy region before the onset of T_g, nor in the value of the rubbery plateau region in the region following T_g. This is an indication that the structure of the polymers has not been significantly disrupted. DMTA analysis of films undergoing exposure at 60°C are in progress.

Similarly, in the case of DSC, very little change was observed in the glass transition temperatures following ambient temperature exposure, as seen in Figs. 8 and 9. The average T_gs obtained from
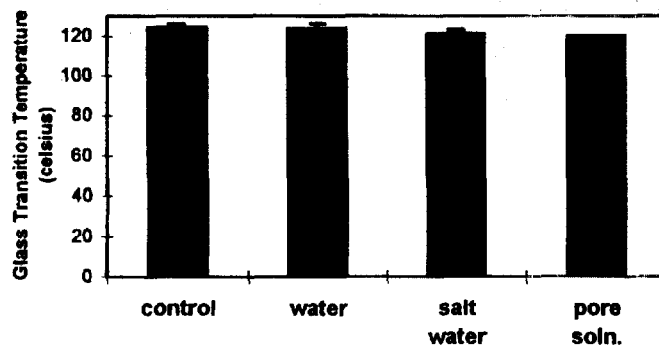

FIG. 7—*Glass transition temperature* T_g *of isopolyester samples measured by dynamic mechanical thermal analysis (DMTA) after 1300 h of immersion in water, salt solution, and concrete pore solution at ambient temperature (uncertainty is equal to ±1 standard deviation).*
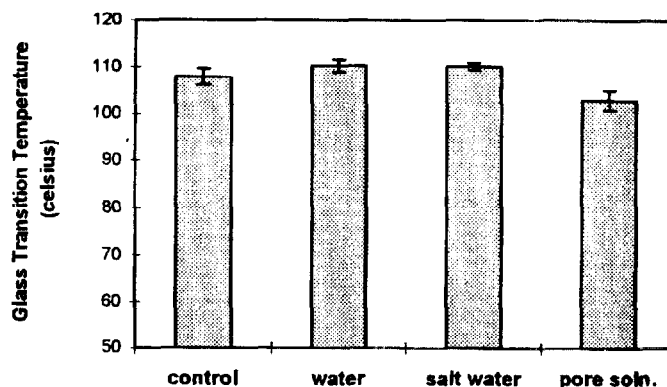

FIG. 8—*Glass transition temperature* T_g *of vinyl ester samples measured by differential scanning calorimetry (DSC) after 1300 h of immersion in water, salt solution, and concrete pore solution at ambient temperature (uncertainty is equal to ±1 standard deviation).*
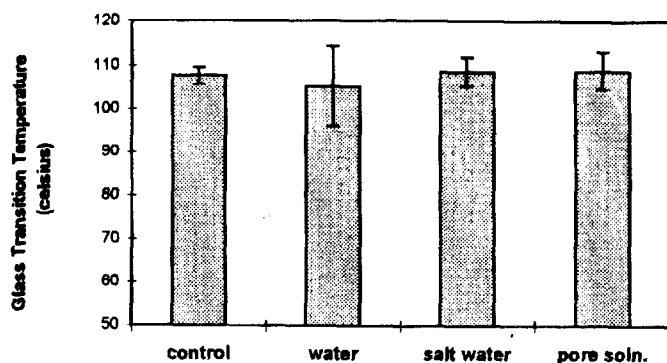
FIG. 9—*Glass transition temperature* T_g *of isopolyester samples measured by differential scanning calorimetry (DSC) after 1300 h of immersion in water, salt solution, and concrete pore solution at ambient temperature (uncertainty is equal to ±1 standard deviation).*

FIG. 11—*Ultimate tensile strengths of isopolyester samples after 1300 h of immersion in water, salt solution, and concrete pore solution at ambient temperature (uncertainty is equal to ±1 standard deviation).*

DSC for the vinyl ester and isopolyester materials are lower than those obtained from DMTA. This is not an anomalous result, since DMTA and DSC measurements are conducted on different time scales (frequencies). DMTA measurements will generally yield higher values for T_g than those obtained by dilatometry or by thermodynamic methods such as DSC [17].

Tensile Testing

Ultimate tensile strengths for the dogbone specimens following environmental exposure are shown in Figs. 10 and 11. Relative to the controls, no significant changes in tensile strength are observed. In the case of polyester specimens exposed to salt water, a large drop in the average strength was observed, but because of the magnitude of the error bars (representing one standard deviation) the differences are not statistically significant. Modulus and elongation values were not calculated at this time due to some uncertainty in the strain measurement technique.

A number of isopolyester and vinyl ester rods reinforced with glass fiber were subjected to salt water and alkaline conditions by Altizer et al. [18]. Following 4800 h of exposure at ambient temperature, little loss in strength was observed for rods exposed to salt water, but decreases in stiffness and strength were observed in rods subjected to alkaline immersion.
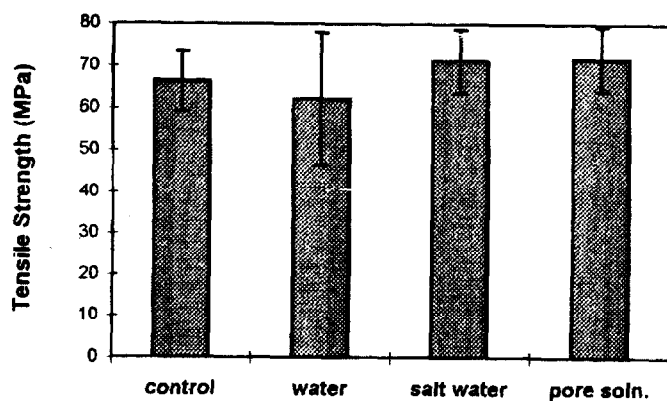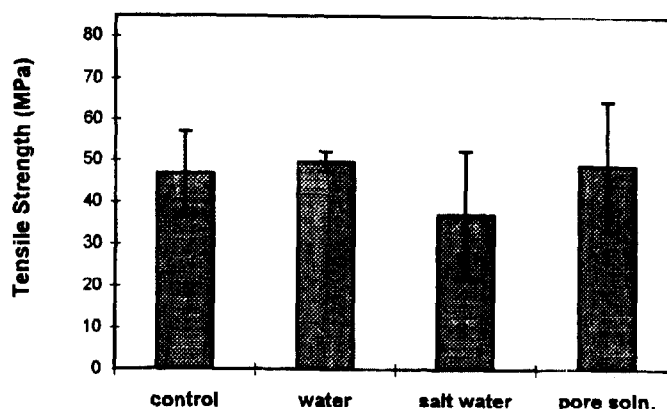
X-Ray Photoelectron Spectroscopy (XPS)

Specimens subjected to UV irradiation for 1200 h showed no changes in bulk properties, as revealed by the results of DMTA analysis that showed no differences between the glass transition temperatures of non-exposed and UV-exposed samples. However, the surface chemical composition showed dramatic changes, as determined by XPS. Table 1 lists atomic concentrations of major elements found in the vinyl ester and isopolyester films before and after UV irradiation. Both the isopolyester and vinyl ester resins are primarily composed of carbon and oxygen. The vinyl ester system contains silicon that originates from the silicone defoamer used in specimen preparation. Following UV exposure, significant increases in the atomic concentration of oxygen was observed. In the case of vinyl ester, silicon was also observed to increase, possibly due to the "blooming" of the silicone defoamer from the bulk up to the surface regions.

Curve-fitted carbon 1s photopeaks are shown in Figs. 12 and 13. For the vinyl ester sample shown in Fig. 12, the photopeak from the non-exposed control can be fitted with a hydrocarbon peak at 285 eV and two smaller at peaks at 286.8 and 289.2 eV, corresponding to hydroxyl or ether functionality (C-O) and carboxylate or ester (O = C-O), respectively. These functional groups most likely originate from the ester linkages present in the original structure. Following exposure, the concentrations of C-O and O = C-O moieties (as shown by their peak heights) increase relative to the main hydrocarbon (C-H) peak. However, when the absolute quantities of C-O and O = C-O linkages are calculated as a function of the total atomic concentration of carbon, which has decreased as a result of UV exposure, an interesting observation is made. The concentration of C-O linkages has decreased at the

FIG. 10—*Ultimate tensile strengths of vinyl ester samples after 1300 h of immersion in water, salt solution, and concrete pore solution at ambient temperature (uncertainty is equal to ±1 standard deviation).*

TABLE 1—*X-ray photoelectron spectroscopy (XPS) atomic concentrations for non-irradiated and UV-irradiated vinyl ester and isopolyester films.*
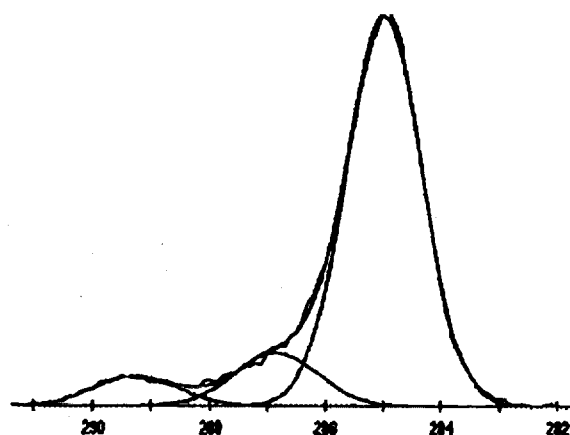
	Atomic Concentration, atomic %		
	Carbon 1s	Oxygen 1s	Silicon 2p
Vinyl ester, non-irradiated	73.3	18.0	8.7
Vinyl ester, UV-irradiated	51.3	29.6	19.1
Isopolyester, non-irradiated	88.5	11.5	—
Isopolyester, UV-irradiated	71.2	28.8	—

NOTE:—Standard deviation of data is typically 0.1 to 0.2 atomic %.

Binding Energy (eV)

(a)
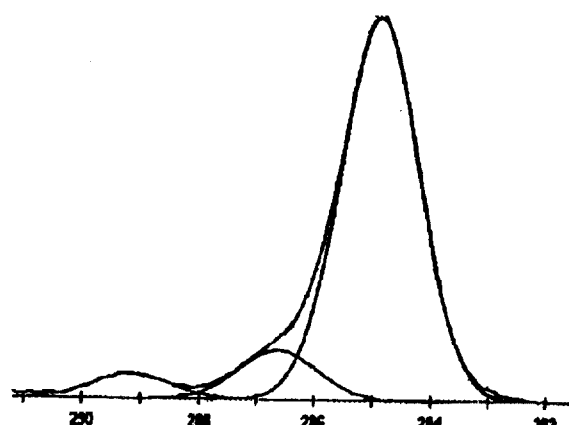

Binding Energy (eV)

(a)
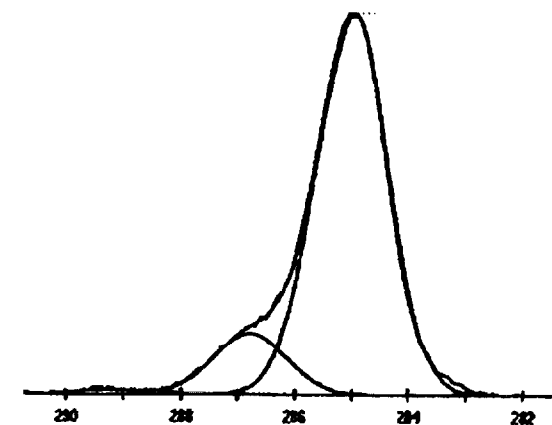
Binding Energy (eV)

(b)

FIG. 12—*Comparison of curve-fitted carbon 1s photopeaks for vinyl ester samples.* (a) *Prior to UV exposure, and* (b) *following 1200 h of UV exposure.*

Binding Energy (eV)

(b)

FIG. 13—*Comparison of curve-fitted carbon 1s photopeaks for isopoly-ester samples.* (a) *Prior to UV exposure, and* (b) *following 1200 h of UV exposure.*
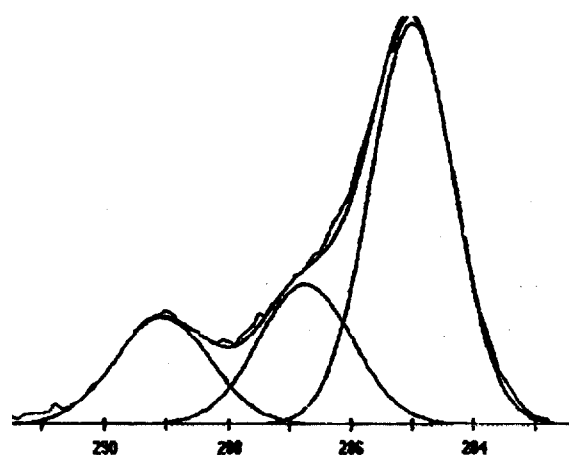
expense of the O = C-O concentration, which has increased, compared to the absolute quantities measured prior to UV exposure. This indicates that the C-O moieties, along with some of the hydrocarbon species, have been further oxidized to ester or carboxylic acid linkages. The fact that no increase in C-O was observed could be evidence that the C-O species in vinyl ester that result from UV irradiation is particularly susceptible to further photo-oxidation and has a short lifetime in the presence of UV.

Dissimilar results are observed for the isopolyester specimens that underwent UV exposure. Figure 13 shows the carbon 1s photopeaks for the exposed and non-exposed specimens. Again, increases in the C-O and O = C-O linkages at 286.6 and 298.2 eV are observed to occur relative to the hydrocarbon peak at 285.0 eV. However, in this instance, calculation of the absolute quantities of carbon species against the total atomic concentration of carbon shows that increases in both C-O and O = C-O occur during UV exposure. These differences in the relative concentrations of C-

O and O = C-O could indicate that different pathways for UV degradation are operative for these two types of polymers.

Atomic Force Microscopy (AFM)

AFM scans of the polymer surfaces following UV exposure are shown in Figs. 14 and 15, along with their corresponding control surfaces. Both polymers display surfaces that are relatively regular and featureless prior to exposure. Following UV exposure, significant amounts of crazing and cratering could be observed, as shown by the dark pits and cracks shown on the AFM images. No such damage could be observed with the naked eye. This drastic change in morphology was also reported by Kaczmarek for a number of thermoplastic polymers following UV exposure [19].

This surface damage parallels the chemical changes observed by XPS and is indicative of a surface oxidation mechanism,
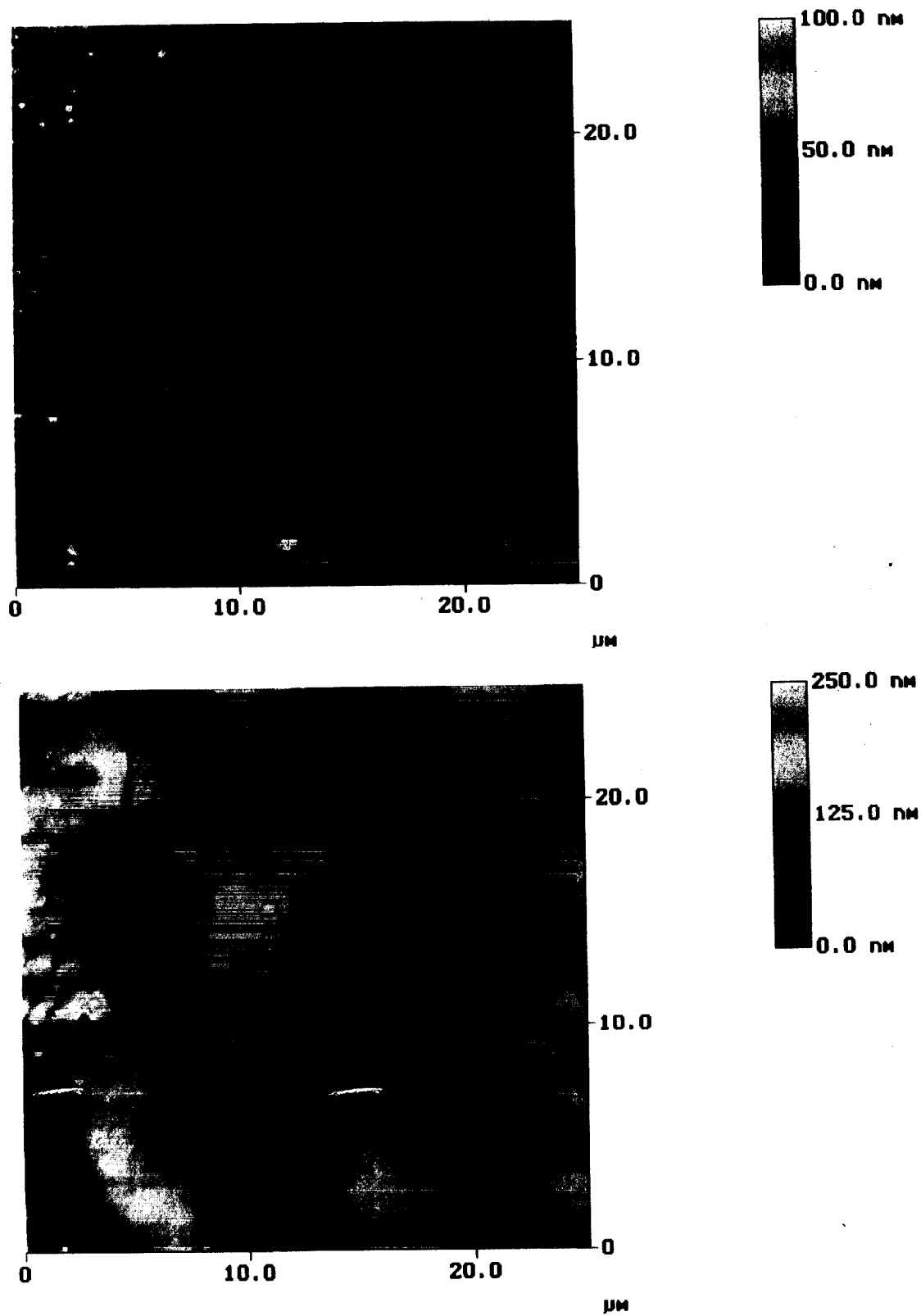
FIG. 14—*Atomic force microscopy (AFM) images for vinyl ester samples.* (a) *Prior to UV exposure, and* (b) *following 1200 h of UV exposure.*
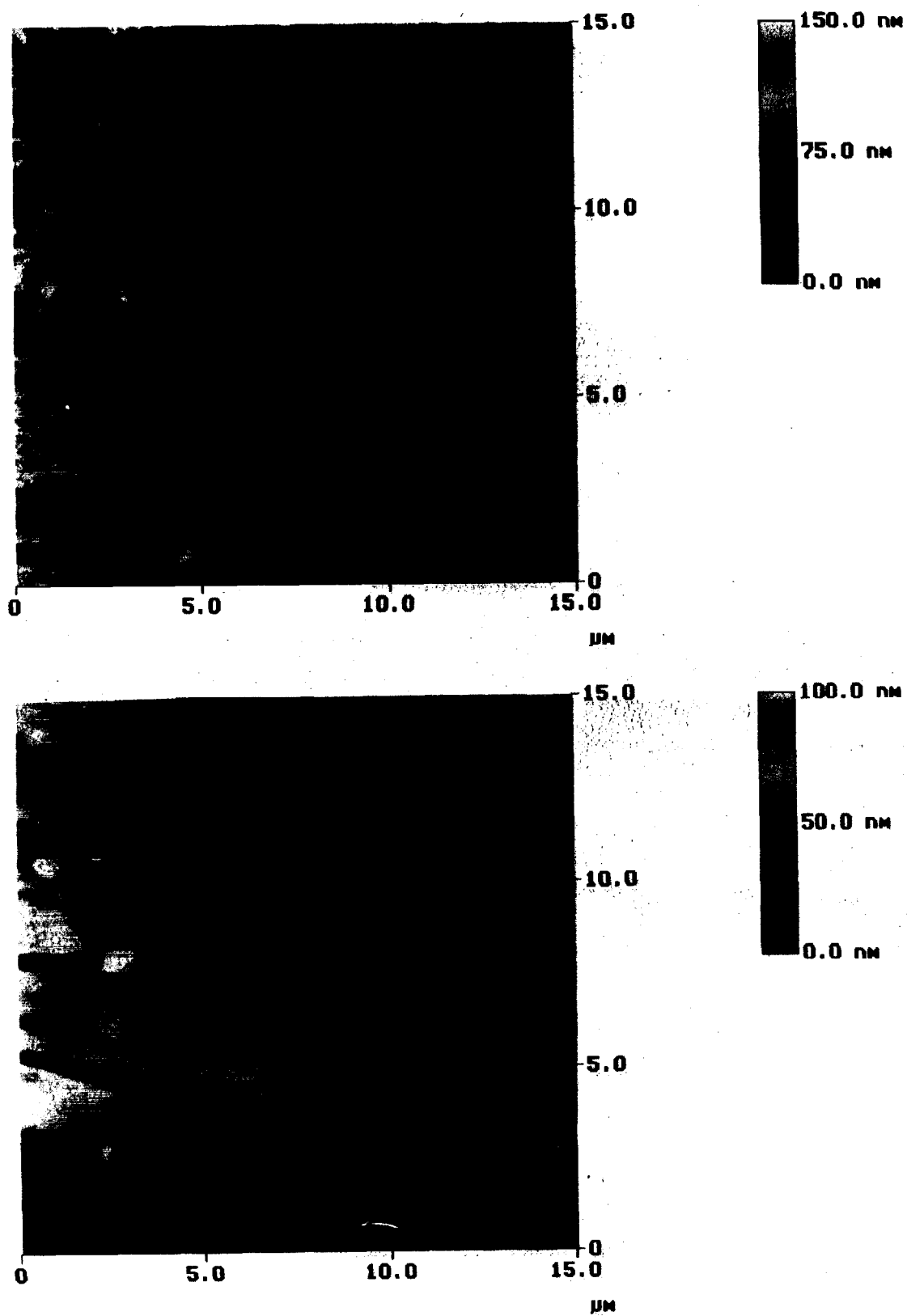
FIG. 15—*Atomic force microscopy (AFM) images for isopolyester samples.* (a) *Prior to UV exposure, and* (b) *Following 1200 h of UV exposure.*

resulting either in embrittlement and cracking due to excessive crosslinking, or surface pitting due to chain scission and the removal of volatile fragments [20]. It is interesting to note that both of these features are observed in the AFM image, possibly pointing to two competing damage mechanisms.

Conclusions

In order to characterize the durability of vinyl ester and polyester materials for use in civil engineering and construction applications, tensile dogbone specimens and free films were exposed to water, salt solution and concrete pore solution. No significant changes were observed in T_g or tensile strengths for vinyl ester and isopolyester resins following 1300 hour immersions in water, salt solution, and concrete pore solution at room temperature. However, 60°C uptake data for the isopolyester resins appears to indicate some type of degradative hydrolysis in alkaline and saline environments. UV exposure results in surface oxidation as evidenced by the increase in oxygen-containing functional groups. Although surface erosion and cracking appear to be similar for both vinyl ester and isopolyester samples, the chemical mechanisms of oxidation appear to differ.

These experiments will be extended to study the effects of 60 and 90°C water, saline and pore solution exposure on the thermophysical and mechanical properties of isopolyester, and vinyl ester resins. In addition, static loading will be included as another environmental variable. Spectroscopic analysis of materials that have undergone water, salt solution, and pore solution exposures will be undertaken. A complete understanding of the degradation mechanisms under various exposure and loading conditions will not only allow material performance to be enhanced, but will facilitate design of valid accelerated aging schemes for service life prediction.

References

[1] AASHTO, The Bottom Line: Transportation Investment Needs—1998-2002, American Association of State Highway and Transportation Officials (AASHTO), 1996.

[2] Dunker, K. F. and Rabbat, B. G., "Why America's Bridges are Crumbling," Scientific American, March 1993, p. 66.

[3] Composite News: Infrastructure, Vol. 34, Oct. 31, 1995.

[4] Civil Engineering Research Foundation, High Performance Construction Materials and Systems: An Essential Program for America and Its Infrastructure, Executive Report 93-5011, 1993.

[5] Giori, C. and Yamauchi, T., "Effects of Ultraviolet and Electron Radiations on Graphite-Reinforced Polysulfone and Epoxy Resins," Journal of Applied Polymer Science, Vol. 29, 1984, p. 237.

[6] Halliwell, S. M., "Weathering of Polymers," RAPRA Review Reports, Vol. 53, 1992.

[7] French, M. A. and Pritchard, G., "Environmental Stress Corrosion of Hybrid Fibre Composites," Composites Science and Technology, Vol. 45, 1992, p. 257.

[8] Shen, C. H. and Springer, G. S., "Effects of Moisture and Temperature on the Tensile Strength of Composite Materials," Environmental Effects on Composite Materials, G. S. Springer, Ed., Technomic Publishing Co., 1981, p. 79.

[9] Boyle, H. C. and Karbhari, V. M., "Bond and Behavior of Composite Reinforcing Bars in Concrete," Polymer-Plastic Technology and Engineering, Vol. 34, No. 5, 1995, p. 697.

[10] American Concrete Institute, "State-of-the Art Report on Fiber Reinforced Plastic (FRP) Reinforcement for Concrete Structures," ACI 440R-96, American Concrete Institute, 1996.

[11] U.S. Government Printing Office, "Composite Materials for Offshore Operations: Proceedings of the First International Workshop," S. S. Wang and D. W. Fitting, Eds., NIST Special Publication 887, U.S. Government Printing Office, 1995.

[12] Christensen, B. J., Mason, T. O., and Jennings, H. M., Journal of the American Ceramic Society, Vol. 75, 1992, p. 939.

[13] Technomic Publishing Co., Inc., Environmental Effects on Composite Materials, Vols. 1, 2, and 3, G. S. Springer, Ed., Technomic Publishing Co., Inc., 1984.

[14] Morri, T., Tanimoito, T., Hanada, H., Maekawa, A., Hirano, T., and Kiyosumi, K., "Weight Changes of a Randomly Oriented GRP Panel in Hot Water," Composites Science and Technology, Vol. 49, 1993, p. 209.

[15] Katsuki, F. and Uomoto, T., "Prediction of Deterioration of FRP Rods Due to Alkali Attack," Non-Metallic (FRP) Reinforcement for Concrete Structures, L. Taerwe, Ed., E and FN Spon, 1995, p. 82.

[16] Byrdson, J. A., Plastics Materials, 5th edition, Chapter 4, Butterworth, 1989.

[17] Aklonis, J. J. and McKnight, W. J., Introduction to Polymer Viscoelasticity, 2nd edition, Wiley Interscience, 1983.

[18] Altizer, S. D., Vijay, P. V., GangaRao, H. V. S., Douglass, N., and Pauer, R., "Thermoset Polymer Performance under Harsh Environments to Evaluate Glass Composite Rebars for Infrastructure Applications," Proceedings from the Composite Institute's 51st Annual Conference and Exposition, 1996, p. 3-C/1.

[19] Kaczmarek, H., "Changes to Polymer Morphology Caused by UV Irradiation: 1. Surface Damage," Polymer, Vol. 37, No. 2, 1996, p. 189.

[20] Ranby, B. and Rabek, J. F., Photodegradation, Photo-Oxidation and Photostabilization of Polymers, John Wiley and Sons, 1975.